Crossed Andreev reflection in a zigzag graphene nanoribbon-superconductor junction

J. Wang and S. Liu

Phys. Rev. B **85**, 035402 — Published 3 January 2012

DOI: 10.1103/PhysRevB.85.035402

Crossed Andreev Reflection in a Zigzag graphene nanoribbon-superconductor junction

J. Wang and S. Liu*

Department of Physics and Astronomy,

California State University, Northridge, CA 91330, USA and

Department of Physics, Southeast University, Nanjing 210096, China

Abstract

We investigate the crossed Andreev reflection (CAR) in a zigzag graphene nanoribbon/superconductor/nanoribbon junction. It is shown that when the zigzag chain number of the ribbon is even and only the zero-energy mode is involved in transport, either the elastic cotunneling or the local Andreev reflection could be entirely suppressed by using a gate voltage whereas a sizeable CAR is achieved. When one of the ribbon leads is magnetized, not only the CAR is exclusive but also the spin state of the CAR transmission is nonlocally controllable. The physical origin is the peculiar valley selection rule in the even zigzag graphene nanoribbon. The ideal Cooper-pair splitting in the proposed device holds for all applied bias in the superconducting energy gap.

PACS numbers: 74.45.+c; 73.23.-b; 74.78.Na

I. INTRODUCTION

The quantum entanglement,[1] describing a physical scenario that the two objects of a quantum state separated in space are strongly correlated, has been attracting much attentions of researchers, not only because it has fundamental research interests in quantum physics, but also it has great application potentials in quantum processes and communications.[2–6] Presently, the realization of the charge or spin entanglement of two electrons remains a major challenge in the solid state physics, even though the polarization entanglement of photons has been implemented in experiment.[7]

A superconductor (S) may be a natural source of Einstein Podolasky Rosen pairs of electrons, as a Cooper pair consists of two electrons that are both spin- and momentum-entangled.[2,8] To split a Cooper pair spatially, the crossed Andreev reflection (CAR) at the normal metal/superconductor interface is indispensable, i.e., an electron (hole) in one of the normal metals is incident into the attached S lead and reflected as a hole (electron) in the other metal. However, the CAR process could be often completely masked by a competing process known as elastic cotunneling (EC) that occurs in the same hybrid S junction, and these two processes have the same transmission coefficients in terms of the lowest-order perturbation approximation,[9] thus necessitating the usage of noise measurement to find fingerprints of the CAR process.[10–13]

Recently, several proposals[14–19] were put forward to find an exclusive CAR by suppressing both the EC and local AR processes. Veldhorst *et al.*[16] have predicted that a 100% fraction of the CAR is possible in a n-type semiconductor/S/p-type semiconductor hybrid junction by making use of the band structure imposed energy filtering; however, the optimal operation requires that the Fermi level is fixed at the bottom of the left conduction band and the

vertex of the right valence band, $E_c = E_v$. Graphene-based devices have also been studied to generate an exclusive CAR by Cayssol[17] and Linder *et al.*[18], and they utilized mainly the zero density of state at the Dirac point to suppress both the EC and local AR. Therefore, a precise bias or gate voltage is needed to modulate the local Fermi energy at the Dirac point. However, it is questionable because any energy fluctuation or spacial density fluctuation could enable the transport to deviate from the Dirac point and the Klein-Gorden paradox[20] or residual conductance makes the EC transmission sizeable.

To avoid fixing precisely a unique parameter to enhance the fraction of the CAR, we propose in this work a perfect CAR device based on the zigzag graphene nanoribbon (ZR) as schematically shown in Fig. 1(a), which can work in a large range of parameters such as bias and gate voltage. The wavefunctions of the electron-like and hole-like particles in the ZR have a definite pseudoparity,[21–26] and they are exactly opposite to each other when the zigzag chain number is even as shown in Fig. 1(b). Accordingly, for an undoped ZR/S junction, the local AR should vanish due to opposite pseudoparities of the incident electron (hole) and reflected hole (electron);[25] however, when a gate voltage (v_g) is applied on the ribbon to shift the site energy, only the electron-like or hole-like zero-energy mode is involved in transport so that the AR will be allowed as long as $ev_g > \Delta$ with Δ the pair potential strength. Therefore, it is possible to split a Cooper pair spatially in a ZR/S/ZR junction by using a gate voltage. Besides, we further observe that the local AR is also prohibited for a magnetized ZR (MZR) as shown in Fig. 1(c), where the spin-up (down) electron band and spin-down (up) hole band are exactly overlapped to each other with opposite pseudoparities. Hence, in a MZR/S/ZR or ZR/S/MZR junction, not only a 100% fraction of CAR can be achieved with vanishing EC and local AR, but also the spin state of the CAR transmission could be controlled entirely by the magnetization of the MZR.

II. FORMULISM

We start from the schematic ZR/S/ZR junction shown in Fig. 1(a), where an S metal deposited on the ZR is grounded, the left ZR and the right ZR are respectively biased V_L and V_R, the width of the ribbon is denoted by the zigzag chain number N, and the length of the S region is La with a the lattice constant. The following Hamiltonian is adopted to describe the system

$$H = \sum_{l\sigma} U_j C^\dagger_{l\sigma} C_{l\sigma} - \sum_{<lm>\sigma} t(C^\dagger_{l\sigma} C_{m\sigma} + c.c.) + \sum_{k\sigma} (\varepsilon_k - \mu) b^\dagger_{k\sigma} b_{k\sigma} + \sum_k (\Delta b^\dagger_{k\uparrow} b^\dagger_{-k\downarrow} + c.c.) + \sum_{<li>\sigma} (t_{li} C^\dagger_{l\sigma} b_{i\sigma} + c.c.), \quad (2.1)$$

where the 1st and 2nd term describe the ZR, $C^\dagger_{l\sigma}(C_{l\sigma})$ is the creation (annihilation) operator at site l with spin σ ($\sigma = \pm = \uparrow\downarrow$), $\langle lm\rangle$ denotes the summation over the nearest neighbor sites, $t = 2.8$ eV is the hopping integral,[27] U_j stands for the lattice site energies of the left ($j = L$), right ($j = R$), and S ($j = S$) ribbon region; the 3rd and 4th terms describe the S metal lead, μ is the chemical potential, and Δ is the superconducting pair potential; the last term is the coupling between the S lead and the ribbon with t_{li} denoting the hopping energy, $b_{i\sigma}$ is the lattice version of the operator $b_{k\sigma}$ in the S lead.

The device in Fig. 1 can be regarded as a three-terminal device that the left ZR, the right ZR, and the S metal leads are connected to the S ribbon region. The current flowing in the left ZR lead can be evaluated from the standard Keldysh formalism

$$I_L = \frac{e}{h} \int dE \, \mathrm{Tr}[H_{i,i+1} G^<_{i+1,i}(E) - G^<_{i,i+1}(E) H_{i+1,i}]_{ee}, \quad (2.2)$$

where $H_{i,i+1}$ is the hopping matrix between two neighboring slices of the ZR with i a unit

slice index, $G^<$ is the lesser Green's function defined as

$$G^<_{lm,\sigma}(t,t') = i \begin{pmatrix} \langle C^+_{m\sigma}(t')C_{l\sigma}(t)\rangle & \langle C_{m\bar{\sigma}}(t')C_{l\sigma}(t)\rangle \\ \langle C^+_{m\sigma}(t')C^+_{l\bar{\sigma}}(t)\rangle & \langle C_{m\bar{\sigma}}(t')C^+_{l\bar{\sigma}}(t)\rangle \end{pmatrix} \tag{2.3}$$

with $\bar{\sigma} = -\sigma$, $H_{i,i+1}$ and $G^<$ are $8N \times 8N$ matrices by taking both the spin and Nambu spaces into account. The trace is carried out over the transverse site and spin space, and the subscript ee stands for the electron component of the Nambu space. According to the Keldysh formula, $G^< = G^r\Sigma^<G^a$, where $G^{r(a)}$ is the retarded (advanced) Green's function and $\Sigma^<$ is the lesser self-energy, the current is reduced to

$$\begin{aligned} I_L = \frac{e}{h}\int dE\, \mathrm{Tr}\{&\Gamma^L_{ee}G^r_{ee}\Gamma^R_{ee}G^a_{ee}(f_L - f_R) + \Gamma^L_{ee}G^r_{eh}\Gamma^L_{hh}G^a_{he}(f_L - \bar{f}_L) + \\ &\Gamma^L_{ee}G^r_{eh}\Gamma^R_{hh}G^a_{he}(f_L - \bar{f}_R) + \Gamma^L_{ee}G^r\Gamma^SG^a(f_L - f_S)\}, \end{aligned} \tag{2.4}$$

where the first term denotes the EC process, the second term describes the local AR process, the 3rd term stands for the CAR, and the last one is the quasiparticle's tunneling term which occurs mainly out of the superconducting energy gap; f_j $(j = L, R, S)$ is the Fermi-Dirac distribution function in the jth lead, $f_{L(R)} = f(E + eV_{L(R)})$ and $\bar{f}_{L(R)} = f(E - eV_{L(R)})$; $\Gamma^j = i(\Sigma^{jr} - \Sigma^{ja})$ represents the linewidth function of the jth lead, $\Sigma^r = [\Sigma^a]^\dagger$ is self-energy and the Green's function of the S region is given by

$$G^r = [E\hat{I} - H_s - \Sigma^L - \Sigma^R - \Sigma^S]^{-1}, \tag{2.5}$$

where H_s is the Hamiltonian of the S ribbon region in the Nambu space and $\hat{I}$ is a unit matrix. The left and right self-energies $\Sigma^{Lr,Rr}$ can be evaluated from the semi-infinite ideal ZR leads, while that of the S lead is given by $\Sigma^S = \sum_{i_a,i_b} t_{l,i_a} g^r_S(i_a,i_b) t^*_{i_b,m}$, where $g^r_S(i_a,i_b)$ is the surface Green's function of the S lead connecting the ZR, and it can be transformed from the bulk S Green's function,[26] $g^r_S(i_a,i_b) = \sum_k e^{i\mathbf{k}(i_a - i_b)} g^r_S(\mathbf{k})$, $i_{a,b}$, same as indices l

and m, denote the ZR lattice site. Note for a conventional s-wave S, the bulk S Green's function is equal to its surface Green's function.[28] For further simplicity, we assume each ZR site in the S region connects independently a 1D S lead as adopted in Ref. 19, it is equivalent to $g_S^r(i_a, i_b) = g_S^r(i_a, i_a)\delta(i_a - i_b)$, thus the self-energy can be analytically obtained as $\Sigma^S = -ig^S(E\hat{I} + \Delta\hat{\sigma}_x)/2\Omega$, with $\Omega = \sqrt{E^2 - \Delta^2}$ at $|E| > \Delta$ and $\Omega = i\sqrt{\Delta^2 - E^2}$ at $|E| < \Delta$. Such approximation of the self-energy of the S lead does not cause a qualitative change to our following numerical results.

III. RESULTS AND DISCUSSIONS

Owing to the valley selection rule,[21–24] the local AR should be prohibited at the interface of the undoped ZR/S junction,[25,26] since the electron-like and hole-like zero-energy states have opposite pseudoparities for an even ZR as shown in the left panel of Fig. 1(b). Nevertheless, the AR can be released by shifting the local Fermi energy of the ZR from the Dirac point, which enables only the electron-like or hole-like zero-energy state contributing to the current. Accordingly, it is possible to split spatially Cooper pairs in a ZR/S/ZR junction by a gate voltage. As shown in the right panel of Fig. 1(b), a positive gate voltage applied on the ZR results in the energy-dispersion shifting downwards, and only the electron-like zero-energy state is involved in transport, so the local AR is allowed now since the electron (e) and hole (h) have the same pseudoparities.

Figure 2 shows numerically obtained EC, AR, and CAR probabilities as a function of the left bias eV_L. In calculations, the zero temperature is considered $T = 0$ K, the pair potential is set as $\Delta = 1$ meV, the linewidth constant of the S lead is set as $g^S = 2\Delta$ while $\Gamma^{L(R)}$ can be calculated directly from a semi-infinite ZR. In Fig. 2(a), the local AR is thoroughly suppressed due to $U_L = 0$, i.e., the Fermi energy in the left ZR is actually

locating at the Dirac point and the injected quasiparticles have an opposite pseudoparity to that of retroflection-quasiparticles, as shown in the left panel of Fig. 1(b). At the right ZR, $U_R = -5\Delta$ is set and only the electron-like zero-energy mode is involved in transport, thus the CAR is allowed $T_{CAR} \neq 0$. Therefore, in such device, the suppression of the local AR and permission of the CAR make it possible to split a Cooper pair in space. For $eV_L < 0$ in Fig. 2(a), all quantities, T_{EC}, T_{AR}, and T_{CAR}, are vanishing because $U_S = -10\Delta$ in the S ribbon region, and the system resembles a *pnn* junction and then the intervalley selection rule blocks the current flowing.[21–23]

Although the local AR in the left lead is prohibited ($T_{AR} = 0$) and the CAR in the right one is allowed ($T_{CAR} \neq 0$) in Fig. 2(a), the EC is also allowed (dot line). In an opposite gate-voltage scheme, $U_L = -5\Delta$ and $U_R = 0$, one can entirely separate the EC and CAR as shown in Fig. 2(b), where at bias $eV_L < 0$, the CAR is allowed ($T_{CAR} \neq 0$) but the EC is prohibited ($T_{EC} = 0$), while the situation is reversed at $eV_L > 0$ that the CAR is zero but the EC is nonzero. Since $U_L < 0$, the left and right ZRs consist a *np* junction for quasiparticles with $E < 0$, so that the EC process would be blocked at $eV_L < 0$ due to the valley selection rule. For $eV_L > 0$, the electrons in both left and right ZRs have the same '+' pseudoparity so the EC can not be blocked, $T_{EC} > 0$, but the hole band in the right ZR has the '-' pseudoparity and thus $T_{CAR} = 0$. It is noted that there is no symmetry between the EC and CAR in magnitude with respect to the bias eV_L whereas the local AR is an even function of eV_L as shown in Fig. 2(b).

The EC and CAR processes can be separated as shown in Fig. 2(b) by setting $U_L = -5\Delta$ and $U_R = 0$, but the local AR is allowed accompanying the CAR, too. So this scheme is also unfavorable to split a Cooper pair. In order to suppress both the EC and AR simultaneously and leave the CAR alone, a magnetized ZR, MZR, shall be introduced to replace either the

left or right ZR lead. Due to the spin splitting, only the electron-like or hole-like zero-energy state will be involved in the AR process as long as the magnetization strength $h > \Delta$, so the T_{EC} and T_{CAR} can be separated as above. Meanwhile, the electron and hole bands of the MZR are exactly overlapped with opposite pseudoparities as shown in Fig. 1(c), thus making the local AR impossible.

The magnetization $\mathbf{h}$ in ZR can be obtained through a magnetic proximity effect and h is about 5 meV estimated in Ref. 28. In calculations, the spin exchange term $\mathbf{h} \cdot \boldsymbol{\sigma}$ replaces the site energy $U_{L(R)}$ in Eq. (1). Figure 3 shows the spin-resolved scattering probabilities, T^{σ}_{EC}, T^{σ}_{AR}, and T^{σ}_{CAR} in the MZR/S/ZR junction. At $eV_L < 0$ in Fig. 3(a), both the EC and local AR are vanishing and only the CAR is nonzero. Meanwhile, the quasiparticles via the CAR process are fully spin-polarized because $T^{\downarrow}_{CAR} = 0$; similarly, the EC particles are also fully spin-polarized ($T^{\downarrow}_{EC} = 0$) at $eV_L > 0$. The reason is that the site energy U_S in the S region ($|U_S| > h > \Delta$) must prohibit one spin-species band of the MZR contributing to current thanks to the valley selection rule. In other words, when U_S is reversed, the spin states of the CAR and EC transmissions are also reversed as well as the applied voltage eV_L, which is shown in Fig. 3(b).

We also plot both $T^{\uparrow}_{CAR}$ and $T^{\uparrow}_{EC}$ as a function of the S ribbon length L in Fig. 4, where the probabilities exhibit a fast oscillation that is related to the formation of resonant transmission levels inside the S region. Since there are two interfaces in the MZR/S/ZR junction, the electron resonant transmission must give rise to the oscillating behaviors of both the EC and CAR coefficients with variation of the length L. The T_{CAR} increases at very short L, then peaks at the superconducting coherence length ξ, and finally decays to zero at $L \gg \xi$. While the EC also exhibits resonant oscillations and decreases monotonously with increase of L as shown in Fig. 4(b). Such oscillating behaviors were also found in the

bulk graphene/S/graphene junction studied in Ref. 17 and 18.

The remarkable aspect of the proposed MZR/S/ZR is that the exclusive CAR is allowed in whole energy gap and meanwhile, both the EC and local AR processes are forbidden entirely. In other words, we do not resort to fixing precisely the bias or gate voltage at a single point to obtain the exclusive CAR as done in Ref. 17 and 18. In fact, the results shown in Fig. 2 and Fig. 3 depend merely on the conditions $U_L(U_R) > \Delta$ and $U_S > h > \Delta$, while it is reasonable for the Δ takes a maximum energy unit and the local Fermi energy $U_S > h$ in the S region is also easily accessible. Only one ZR lead is magnetized so that the spin entanglement is not destroyed unlike that in the HM/S/HM junction[14] (HM: half metal), where both spin states in two HM leads are fixed to achieve an exclusive CAR. Similarly, the exclusive CAR is also attainable in the ZR/S/MZR junction, where the local conductance in the left ZR is fully spin-polarized and can be controlled by nonlocal magnetization of the right MZR. To implement the proposed CAR device, the prefect even ZR in nanoscale is a prerequisite, so the first energy-level difference $\delta E \sim t\pi/N$ of the ZR is large enough to insure only the zero-energy edge states involved in transport. For a 50 nm ZR in width, $\delta E \sim 50$ meV, which is much larger than the pertained quantities U_i, Δ, and h used in calculations. Moreover, the nanosize ZR has already been fabricated successfully in experiments.[30–32]

IV. CONCLUSION

To summarize, we have investigated the nonlocal quantum transport in a ZR/S/ZR hybrid junction. It is shown that either the EC or local AR can be suppressed with a gate voltage applied on one ZR lead, and when one of the ZR leads is magnetized, an exclusive CAR is possible for all applied bias voltages with full suppression of both the EC and AR. The spin state of the nonlocal conductance dominated merely by the CAR could be modulated by

the local magnetization. The basic mechanism behind this effect is the peculiar ZR band structure and the valley selection rule. Finally, since both undoped and magnetized even-ZR block the local AR thoroughly, the proposed device may serve as a very efficient Andreev beam splitter.

---

* Electronic address: su.liu.20@csun.edu

[1] J. M. Raimond, M. Brune, and S. Haroche, Rev. Mod. Phys. **73**, 565 (2001); L. Amico, R. Fazio, A. Osterloh, and V. Vedral, Rev. Mod. Phys. **80**, 517 (2008).

[2] P. Recher, E.V. Sukhorukov, and D. Loss, Phys. Rev. B **63**, 165314 (2001).

[3] G. B. Lesovik, T. Martin, and G. Blatter, Eur. Phys. J. B **24**, 287 (2001).

[4] N. M. Chtchelkatchev, G. Blatter, G. B. Lesovik, T. Martin, Phys. Rev. B **66**, 161320(R) (2002).

[5] K. V. Bayandin, G. B. Lesovik, and T. Martin, Phys. Rev. B **74**, 085326 (2006).

[6] S. Kawabata, J. Phys. Soc. Jpn. **70**, 1210 (2001).

[7] A. Aspect, J. Dalibard, and G. Roger, Phys. Rev. Lett. **49**, 1804 (1982).

[8] G. Burkard, D. Loss, and E.V. Sukhorukov, Phys. Rev. B **61**, R16303 (2000)

[9] G. Falci, D. Feinberg, and F. W. J. Hekking, Europhys. Lett. **54**, 255 (2001).

[10] D. Beckmann, H. B. Weber and H.v. Lohneysen, Phys. Rev. Lett. **93**, 197003 (2004).

[11] S. Russo, M. Kroug, T. M. Klapwijk and A. F. Morpurgo, Phys. Rev. Lett. **95**, 027002 (2005).

[12] P. Cadden-Zimansky and V. Chandrasekhar, Phys. Rev. Lett. **97**, 237003 (2006).

[13] C. Benjamin and J. K. Pachos, Phys. Rev. B **78**, 235403 (2008).

[14] G. Deutscher and D. Feinberg, Appl. Phys. Lett. **76**, 487 (2000).

[15] J. Nilsson, A. R. Akhmerov, and C. W. J. Beenakker, Phys. Rev. Lett. **101**, 120403 (2008).

[16] M. Veldhorst and A. Brinkman, Phys. Rev. Lett. **105**, 107002 (2010).

[17] J. Cayssol, Phys. Rev. Lett. **100**, 147001 (2008).

[18] J. Linder, M. Zareyan, and A. Sudbø, Phys. Rev. B **80**, 014513 (2009).

[19] R. Mélin, F. S. Bergeret, A. Levy Yeyati, Phys. Rev. B **79**, 104518 (2009); A. Levy Yeyati, F. S. Bergeret, A. Martin-Rodero, and T. M. Klapwijk, Nat. Phys. **3** 455 (2007).

[20] M. I. Katsnelson, K. S. Novoselov, and A. K. Geim, Nat. Phys. **2**, 620 (2006).

[21] A. Rycerz, J. Tworzydlo, and C. W. J. Beenakker, Nat. Phys. **3**, 172 (2007).

[22] A. R. Akhmerov, J. H. Bardarson, A. Rycerz, and C. W. J. Beenakker, Phys. Rev. B **77**, 205416 (2008).

[23] A. Cresti, G. Grosso, and G. P. Parravicini, Phys. Rev. B **77**, 233402 (2008).

[24] K. Wakabayashi and T. Aoki, Int. J. Mod. Phys. B **16**, 4897 (2002).

[25] D. Rainis, F. Taddei, F. Dolcini, M. Polini, and R. Fazio, Phys. Rev. B **79**, 115131 (2009).

[26] J. Wang, L. Zhang, and K. S. Chan, Phys. Rev. B **83**, 125425 (2011).

[27] L. Pisani, J. A. Chan, B. Montanari, and N. M. Harrison, Phys. Rev. B **75**, 064418 (2007).

[28] M. P. Samanta and S. Datta, Phys. Rev. B **57**, 10972 (1998).

[29] H. Haugen, D. Huertas-Hernando, and A. Brataas, Phys. Rev. B **77**, 115406 (2008).

[30] Z. Shi, R. Yang , L. Zhang, Y. Wang, D. Liu, D. Shi, E. Wang, and G. Zhang, Adv. Mater. **23**, 3061 (2011).

[31] L. C. Campos, V. R. Manfrinato, J. D. Sanchez-Yamagishi, J. Kong, and P. Jarillo-Herrero, Nano Lett. **9**, 2600 (2009).

[32] X. Jia, M. Hofmann, V. Meunier, B. G. Sumpter, J. Campos-Delgado, J. M. Romo-Herrera, H. Son, Y. Hsieh, A. Reina, J. Kong, M. Terrones, M. S. Dresselhaus, Science **323**, 1701 (2009).

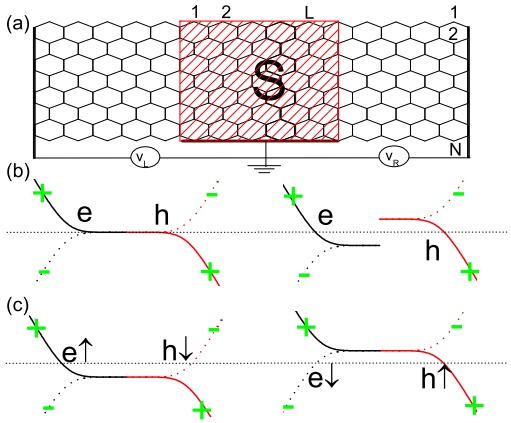

FIG. 1: (Color online) (a) An overview of the setting from the top. A normal superconductor lead (shadow S) on the top of the ZR is grounded and divides the ZR into three regions: the left, S, and right ZR regions; the left and right ZRs are respectively applied with voltage V_L and V_R. (b) Electron and hole energy-dispersions of the edge states in the nonmagnetic even ZR. The hole band 'h' is obtained as a mirror image of the electron band 'e' over the Fermi level (horizontal dot line), '+' and '-' denote respectively the even and odd pseudoparity of the edge states. The left and right panels stand for the situations without and with a gate voltage applied on the ribbon. (c) Electron and hole energy-dispersion of a magnetized even ZR. The spin-up (down) electron band overlaps with spin-down (up) hole band with opposite pseudoparities, and the spin exchange energy causes to a shift of the Dirac point from the Fermi level.

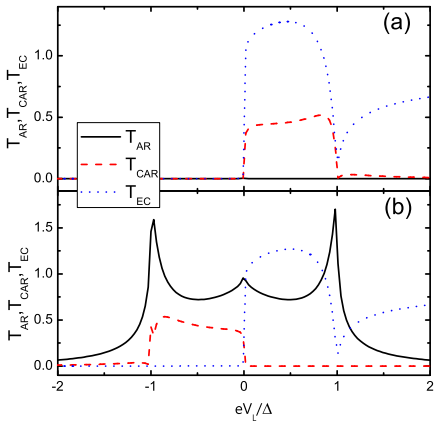

FIG. 2: (Color online) Plot of the AR, CAR, and EC transmission coefficients versus the bias voltage eV_L applied on the left ZR. The solid, dash , and dot lines represent the AR, CAR, and EC processes, respectively. Parameters are $eV_R = 0$, $L = 40$, $U_S = -10$ meV, $U_L = 0$, $U_R = -5$ meV in the upper panel (a), and $U_L = -5$ meV, $U_R = 0$ in the lower panel (b).

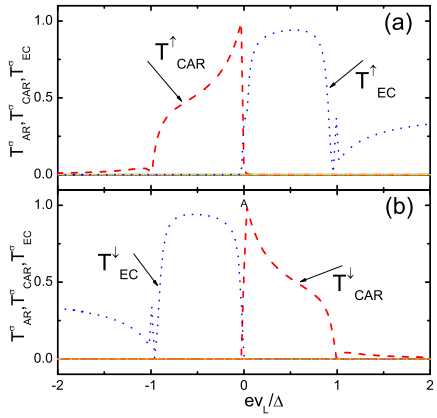

FIG. 3: (Color online) Plot of the spin-resolved AR, CAR, and EC transmission coefficients versus the bias voltage eV_L applied on the left ZR. Only $T^{\uparrow}_{CAR}$ and $T^{\uparrow}_{EC}$ in (a) and $T^{\downarrow}_{CAR}$ and $T^{\downarrow}_{EC}$ in (b) are nonzero while all other quantities are vanishing. Parameters are $eV_R = 0$, $L = 40$, $U_L = U_R = 0$, $h = 5$ meV, $U_S = -10$ meV in (a), and $U_S = 10$ meV in (b).

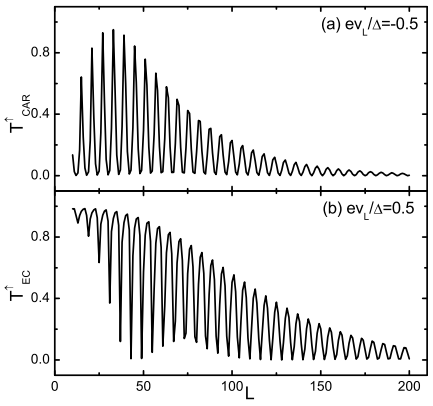

FIG. 4: Spin-dependent CAR (a) and EC (b) transmission coefficients versus the S region length L. Parameters are $eV_R = 0$, $U_L = U_R = 0$, $h = 5$ meV, $U_S = -10$ meV, $eV_L = -0.5\Delta$ in (a) and $eV_L = 0.5\Delta$ in (b).